

UCSF

UC San Francisco Previously Published Works

Title

Substituted 4-methylcoumarin inhibitors of SLC26A3 (DRA) for treatment of constipation and hyperoxaluria.

Permalink

<https://escholarship.org/uc/item/01f1s2gf>

Journal

MedChemComm, 15(5)

Authors

Ahmadi, Maria

De Souza Goncalves, Livia

Verkman, Alan

et al.

Publication Date

2024-05-22

DOI

10.1039/d3md00644a

Peer reviewed

RESEARCH ARTICLE



Cite this: *RSC Med. Chem.*, 2024, 15, 1731

Substituted 4-methylcoumarin inhibitors of SLC26A3 (DRA) for treatment of constipation and hyperoxaluria†

Maria Ahmadi,^a Livia de Souza Goncalves,^b Alan S. Verkman,^c
Onur Cil^{†*b} and Marc O. Anderson^{†*a}

SLC26A3, also known as downregulated in adenoma (DRA), is an anion (Cl^- , HCO_3^- and oxalate) exchanger in the luminal membrane of intestinal epithelial cells. Loss of DRA function in mice and humans causes congenital chloride-losing diarrhea and reduces urinary excretion of oxalate, a major constituent of kidney stones. Thus, inhibition of DRA is a potential treatment approach for constipation and calcium oxalate kidney stones. High-throughput screening previously identified 4,8-dimethylcoumarins (**4a–4c**) as DRA inhibitors, with lead candidate **4b** having an IC_{50} of 40–50 nM for DRA inhibition. Here, we explored the effects of varying substituents at the 8-position, and replacing 8-methyl by 5-methyl (**4e–4h**). A focused library of 17 substituted compounds (**4d–4t**) was synthesized with good yield and purity. Compounds were tested for DRA inhibition potency using Fischer rat thyroid cells stably expressing DRA and a halide-sensitive YFP. Structure–activity analysis revealed that 8-bromo- (**4m–4p**) and 8-fluoro-coumarins (**4q–4t**) were slightly less potent than the corresponding 8-chloro analogs, demonstrating that the size of methyl or chloro substituents at the coumarin 8 position affects the potency. An analog containing 8-chlorocoumarin (**4k**) had ~2-fold improved potency (IC_{50} 25 nM) compared with the original lead candidate **4b**. 5,8-Dimethylcoumarins were active against DRA, but with much lower potency than 4,8-disubstituted coumarins. In mice, orally administered **4k** at 10 mg kg^{-1} reduced constipation and normalized stool water content in a loperamide-induced constipation model with comparable efficacy to **4b**. Pharmacokinetic analysis of orally administered **4k** at 10 mg kg^{-1} in mice indicated serum levels of >10 μM for at least six hours after single dose. This study expands SAR knowledge of 4,8-disubstituted coumarin inhibitors of DRA as novel drug candidates for constipation and kidney stones.

Received 17th November 2023,
Accepted 27th February 2024

DOI: 10.1039/d3md00644a

rsc.li/medchem

Introduction

Constipation is a common disease caused by a wide variety of factors, with a prevalence of 15% in the US and worldwide.^{1,2} Constipation is commonly treated with over-the-counter laxatives as well as prescription drugs, albeit often with limited efficacy.^{2,3} There remains an unmet clinical need for constipation treatments with novel mechanisms of action.

Kidney stone disease affects 9% of the US population and 1–13% of the global population⁴ with a high recurrence rate

of 40–50% in 5 years.^{4,5} To prevent stone recurrence, lifestyle changes and preventive medical treatment are used.⁶ Hyperoxaluria is a major risk factor for calcium oxalate stones,⁷ the most common type constituting 2/3 of all kidney stones.⁸ Currently, medical treatment options for kidney stones are limited and there are no approved treatments for hyperoxaluria.⁹

SLC26A3 (also known as “down regulated in adenoma” or DRA) is an anion exchanger for chloride, HCO_3^- and oxalate.^{10–12} It is mainly expressed in the luminal membrane of epithelial cells in the colon, the site of final stool dehydration and dietary oxalate absorption.¹³ DRA loss-of-function mutations cause congenital chloride-losing diarrhea (CLD) in humans,¹⁴ with a similar phenotype in mice.¹⁵ In addition, *slc26a3* knockout mice¹⁶ and CLD patients have 50–70% reduced urinary oxalate excretion.^{6,17} Thus, DRA inhibitors are drug candidates with a novel mechanism of action for constipation and hyperoxaluria.

Our group identified first-in-class DRA inhibitors by high-throughput screening^{18–20} and follow-on medicinal chemistry.

^a Department of Chemistry and Biochemistry, San Francisco State University, San Francisco, CA, USA. E-mail: marc@sfsu.edu

^b Department of Pediatrics, University of California, San Francisco, San Francisco, CA, USA. E-mail: onur.cil@ucsf.edu

^c Department of Medicine, University of California, San Francisco, San Francisco, CA, USA

† Electronic supplementary information (ESI) available. See DOI: <https://doi.org/10.1039/d3md00644a>

‡ Contributed equally.

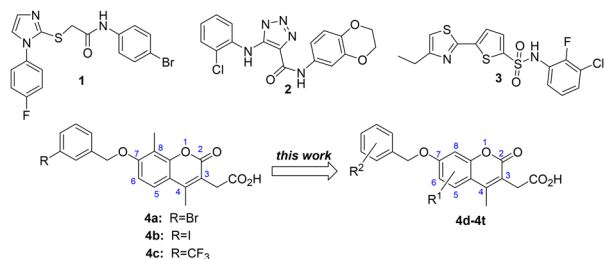


Fig. 1 Previously reported small molecule inhibitors of DRA and newly developed inhibitors (**4d–4t**).

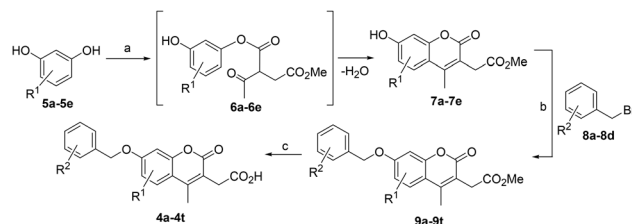
DRA inhibitors previously identified by our group are shown in Fig. 1, which include acetamide-thioimidazoles (**1**), triazoleamides (**2**), and thiazole-thiophenesulphonamides (**3**). A lead class of inhibitors are 4,8-dimethylcoumarins (**4**) and the lead candidate 3-iodobenzyloxy-4,8-dimethylcoumarin-3-acetic acid (**4b**) was identified by studying modifications of the benzyl group and side chains. **4b** had an IC_{50} of 40 nM for DRA inhibition and good efficacy in mouse models of constipation^{18,19} and hyperoxaluria.⁶ Previous medicinal chemistry efforts focused on variation of the benzyloxy group on C7 and of the linked carboxylic acid group.¹⁹ However, the effects of varying the central coumarin scaffold were not explored previously. Although **4b** is a drug candidate with good efficacy in mouse models, it had some potential liabilities. Aromatic iodides, analogous to the benzyloxy group of potent inhibitor **4b**, have been shown to be hepatotoxic and deplete GSH.²¹ The commonly used anti-arrhythmia drug amiodarone contains an aryl diiodide moiety, and has been found to induce photosensitivity and hyperpigmentation,²² as well as hepatotoxicity that appears associated with accumulation of iodine in the liver.²³ These concerns provide rationale to identify lead candidates that lack the aromatic iodide, but with maintained or improved *in vitro* and *in vivo* activity.

By replacement of 8-methyl at R^1 (original scaffold) with 5-methyl, 8-chloro, 8-bromo, or 8-fluoro, here we explored the key structural features of the 4,8-dimethylcoumarin scaffold important for DRA inhibition. For each variation at R^1 , we also explored 3-Br, 3-I, 3-(CF_3) and 3-(CF_2H) at the R^2 position. By iteratively exploring the R^1 and R^2 positions, this study presents a library of 16 compounds with novel coumarins (**4e–4t**), as well as one difluoromethyl analog of the original 4,8-dimethylcoumarin scaffold (**4d**), for a total of 17 new inhibitor candidates. The central goal of this study is to explore the steric and electronic chemical space of the central coumarin scaffold for DRA inhibition and test the best candidate *in vivo* in mice.

Results and discussion

Synthesis of substituted 4-methylcoumarin compounds

Compounds were prepared using the synthetic strategy shown in Scheme 1. The synthesis begins with the Pechmann condensation reaction where commercially obtained



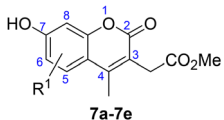
Scheme 1 Synthesis of 4,8-dimethylcoumarin analogues. Reagents and conditions: (a) substituted resorcinol (1.0 eq.), dimethyl acetylsuccinate (1.0 eq.), H_2SO_4 (2.8 eq.), (rt, overnight); (b) K_2CO_3 (2.0 eq.), anhydrous acetone (1.0 eq.), (reflux, overnight); (c) NaOH (4.0 eq.), MeOH (1.0 eq.), (reflux, 2–3 h).

resorcinols (**5a–5e**) were reacted with the β -keto ester dimethyl acetylsuccinate. Sulfuric acid (H_2SO_4) was used as a solvent and reactant, which mediates acid-catalyzed transesterification to generate putative intermediates **6a–6e**. Lastly, electrophilic aromatic substitution and the loss of water lead to the final 5- or 8-substituted 4-methylcoumarin (**7a–7e**). The synthesis of **7a** and its alkylation with benzyl halides (**8a–8c**) to generate intermediates (**9a–9c**) and final products (**4a–4c**) was reported previously,¹⁹ and served as the basis for other substituted coumarin analogs reported herein. The inhibitor candidate products were typically off-white or lightly pink solids. Pechmann products (**7a–7e**) could usually be purified by trituration using hexane and ethyl acetate solution, to yield crystalline products that were homogenous by NMR and ESI-LCMS (>95% purity). The composition of coumarins prepared by Pechmann condensation (**7a–7e**), typically isolated in fair yields, is reported in Table 1.

Next, the substituted 4-methylcoumarins (**7a–7e**) were reacted with substituted benzyl bromides (**8a–8d**) to generate coumarin benzyl ethers (**9a–9t**), through alkylation. The reaction typically yielded white crystalline products that were contaminated by substituted benzyl bromides, but the products could be conveniently purified by trituration. We also found that in case the benzyl ethers were not quantitatively pure, the materials could be pushed to the subsequent ester hydrolysis reaction, where crystallization to pure final products was easily accomplished. The composition of the library and yields for the benzyl alkylation reactions are reported in Table 2.

Finally, the substituted coumarin methyl esters (**9a–9t**) were hydrolyzed *via* base-mediated saponification to form the carboxylic acid final products (**4a–4t**). To avoid unintentional Fischer esterification during acidic aqueous workup, we included an evaporation step (rotary evaporator) prior to addition of aqueous acid. Final compounds were isolated as crystalline solids with high yields and purities (Table 3). In total $5 \times 4 = 20$ inhibitor candidates were prepared by variations at the R^1 and R^2 positions, with compounds **4d–4t** not having been reported previously. The structure and purity (>95%) of the final products were confirmed by NMR and ESI-LCMS (UV absorption detection at 254 nm), with representative compounds confirmed by HRMS.

Table 1 Synthesis yields of substituted 4-methylcoumarin reactions (5 → [6] → 7); yields (%) are of the isolated or purified products. Purity of compounds was >95% based on HPLC-LCMS analysis at 254 nm, and the absence of impurities was confirmed by ¹H NMR spectra

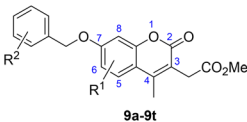


Product hydroxy coumarin	Starting resorcinol	R ¹	Isolated yield (%)
7a	5a	8-(CH ₃)	63
7b	5b	5-(CH ₃)	42
7c	5c	8-Cl	16
7d	5d	8-Br	43
7e	5e	8-F	29

DRA inhibition potency of substituted 4-methylcoumarins

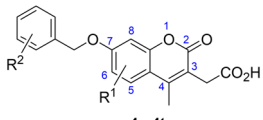
The 4-methylcoumarin carboxylic acid inhibitors (**4a–4t**) were evaluated for DRA inhibition using a YFP-fluorescence assay as previously described.¹⁸ The IC₅₀ values for compounds **4a–4p** are provided in Table 4. Compounds (**4a–4c**) based on a 4,8-dimethylcoumarin scaffold were reported previously¹⁹ and serve as a benchmark to evaluate new molecules. Comparing previous inhibitor **4c** (R² = 3-CF₃) with new inhibitor **4d** (R² = 3-CF₂H) the difference in IC₅₀ is substantial, indicating that the removal of a single fluorine from the substituted benzyl group dramatically reduces

Table 2 Synthesis yields for coumarin benzyl ethers (7 + 8 → 9). Yields (%) are of the isolated or purified products. Purity of compounds was >95% based on HPLC-LCMS analysis at 254 nm, and the absence of impurities was confirmed by ¹H-NMR spectra



Product coumarin methyl ester	Starting hydroxy coumarin	R ¹	R ²	Isolated % yield
9a	7a	8-(CH ₃)	3-Br	81
9b	7a	8-(CH ₃)	3-I	100
9c	7a	8-(CH ₃)	3-(CF ₃)	80
9d	7a	8-(CH ₃)	3-(CF ₂ -H)	55
9e	7b	5-(CH ₃)	3-Br	90
9f	7b	5-(CH ₃)	3-I	85
9g	7b	5-(CH ₃)	3-(CF ₃)	60
9h	7b	5-(CH ₃)	3-(CF ₂ -H)	77
9i	7c	8-Cl	3-Br	56
9j	7c	8-Cl	3-I	63
9k	7c	8-Cl	3-(CF ₃)	55
9L	7c	8-Cl	3-(CF ₂ -H)	79
9m	7d	8-Br	3-Br	58
9n	7d	8-Br	3-I	43
9o	7d	8-Br	3-(CF ₃)	72
9p	7d	8-Br	3-(CF ₂ -H)	59
9q	7e	8-F	3-Br	72
9r	7e	8-F	3-I	77
9s	7e	8-F	3-(CF ₃)	94
9t	7e	8-F	3-(CF ₂ -H)	72

Table 3 Synthesis yields for benzyl acid (9 → 4); yields (%) are of isolated or purified products. Purity of compounds was >95% based on HPLC-LCMS analysis at 254 nm, and the absence of impurities was confirmed by ¹H-NMR spectra

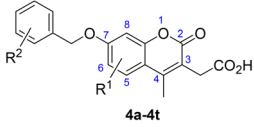


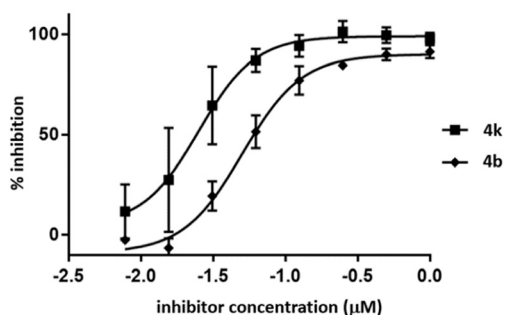
Final product	Starting coumarin methyl ester	R ¹	R ²	Final product % yield
4a	9a	8-(CH ₃)	3-Br	60
4b	9b	8-(CH ₃)	3-I	37
4c	9c	8-(CH ₃)	3-(CF ₃)	81
4d	9d	8-(CH ₃)	3-(CF ₂ -H)	42
4e	9e	5-(CH ₃)	3-Br	35
4f	9f	5-(CH ₃)	3-I	42
4g	9g	5-(CH ₃)	3-(CF ₃)	90
4h	9h	5-(CH ₃)	3-(CF ₂ -H)	100
4i	9i	8-Cl	3-Br	67
4j	9j	8-Cl	3-I	28
4k	9k	8-Cl	3-(CF ₃)	95
4L	9L	8-Cl	3-(CF ₂ -H)	73
4m	9m	8-Br	3-Br	85
4n	9n	8-Br	3-I	38
4o	9o	8-Br	3-(CF ₃)	75
4p	9p	8-Br	3-(CF ₂ -H)	95
4q	9q	8-F	3-Br	58
4r	9r	8-F	3-I	55
4s	9s	8-F	3-(CF ₃)	97
4t	9t	8-F	3-(CF ₂ -H)	95

potency. Also, repositioning the methyl group from the coumarin 8-position (**4a–4d**) to the 5-position (**4e–4h**) greatly reduces the inhibitory potency against DRA, indicating a preference for 4,8-disubstituted coumarins.

Compounds **4i–4L** based on 8-chlorocoumarin were similarly potent to 8-methylcoumarins **4a–4d**, which could be expected due to the isosteric relationship between methyl and chloro. Curiously, in the case of the 8-chlorocoumarins, when considering benzyl substitution (R²), it appears that 3-bromobenzyl (**4i**), 3-iodobenzyl (**4j**), and 3-difluoromethyl (**4L**) appear more potent than the corresponding 8-methylcoumarin analogs (**4a**, **4b**, and **4d**, respectively). However, the most potent inhibitor based on 8-chlorocoumarin **4k** (R² = CF₃) seems to match the analogous 8-methylcoumarin inhibitor (**4c**) also containing this benzyl substituent, both with an IC₅₀ of 25 nM. Compounds **4m–4p** that contain 8-bromocoumarin were less potent than the corresponding 8-chloro or 8-methylcoumarin analogs. This observation suggested that smaller substituents at the 8-position might be advantageous, which led us to synthesize the corresponding 8-fluorocoumarins (**4q–4t**). However, the 8-fluorocoumarins were not as potent as the 8-chloro derivatives (**4i–4L**), but more potent than 8-bromocoumarins (**4m–4p**). Overall, in terms of potency it seems that 8-chloro is the best followed by 8-fluoro and 8-bromo. This can be due to their size with 8-chloro fitting and the other two being either too large (8-bromo) or too small (8-fluoro) to make complementary interactions with the binding site. The concentration dependence of 8-chlorocoumarin

Table 4 DRA inhibition of compounds (**4a–4t**). IC₅₀ (μM) for inhibition of DRA anion conductance using a fluorescence plate reader assay (*n* = 3)

 4a–4t			
Final product	R ¹	R ²	IC ₅₀ (nM)
4a	8-(CH ₃)	3-Br	140 ± 20
4b	8-(CH ₃)	3-I	50 ± 3
4c	8-(CH ₃)	3-(CF ₃)	25 ± 10
4d	8-(CH ₃)	3-(CF ₂ H)	320
4e	5-(CH ₃)	3-Br	560
4f	5-(CH ₃)	3-I	500
4g	5-(CH ₃)	3-(CF ₃)	900
4h	5-(CH ₃)	3-(CF ₂ H)	829
4i	8-Cl	3-Br	86 ± 14
4j	8-Cl	3-I	27 ± 2
4k	8-Cl	3-(CF ₃)	25 ± 4
4L	8-Cl	3-(CF ₂ H)	212 ± 20
4m	8-Br	3-Br	87 ± 14
4n	8-Br	3-I	132 ± 30
4o	8-Br	3-(CF ₃)	131 ± 30
4p	8-Br	3-(CF ₂ H)	345 ± 25
4q	8-F	3-Br	78 ± 7
4r	8-F	3-I	67 ± 7
4s	8-F	3-(CF ₃)	87 ± 6
4t	8-F	3-(CF ₂ H)	274 ± 22

**Fig. 2** Concentration dependence of **4k** and **4b** for inhibition of DRA.

inhibitor **4k** for DRA inhibition is shown in Fig. 2, compared with previously identified lead candidate **4b**.

Efficacy of **4k** in a mouse constipation model

As previously done for earlier DRA inhibitors,^{18,19} **4k** was tested for its efficacy in a loperamide-induced model of constipation in mice (Fig. 3A). In this model, loperamide causes severe constipation as evidenced by reduced stool weight, pellet number and water content. Orally administered **4k** at 10 mg kg⁻¹ improved the stool weight, pellet number and stool water content in loperamide-treated mice, with comparable efficacy to **4b** (Fig. 3B), though mildly greater improvement in stool water content. Single dose **4k** administration at 10 mg kg⁻¹ produced serum levels >10 μM for at least six hours (Fig. 4). Animal experiments were performed in accordance with the Guide for the Care and Use of Laboratory Animals by the National Institutes of Health and approved by the UCSF Institutional Animal Care and Use Committee.

Discussion

Here, we synthesized a focused library of DRA inhibitors and explored variations of the central 4,8-dimethylcoumarin scaffold. The 8-chloro-4-methylcoumarin scaffold showed a comparable potency with the previous 4,8-dimethylcoumarin compounds. Of the new compounds, 8-chloro-4-methylcoumarin **4k** (*R*² = 3-CF₃) matched the potency of previous **4c** based on 4,8-dimethylcoumarin with the same *R*², with an IC₅₀ of 25 nM. However, we previously chose the less potent 4,8-dimethylcoumarin **4b** (*R*² = 3-iodo, IC₅₀ = 40 nM) as a lead candidate due to better *in vivo* efficacy than **4c**.¹⁹ The aryl iodide present in **4b** had some potential concerns about toxicity.^{21–23} Here, we report that 8-chlorocoumarin inhibitor **4k** has a better potency than **4b**, while maintaining *in vivo* efficacy, and eliminating the potential liability of an aryl iodide. The rationale for replacement of 8-methyl with 8-chloro is to prevent possible P450-mediated metabolic oxidation reactions of aromatic

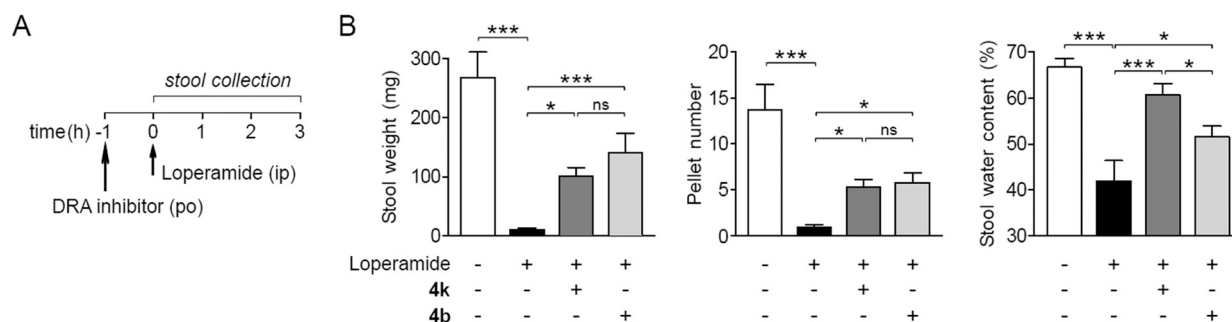


Fig. 3 Efficacy of **4k** (newly identified) versus **4b** (previous lead) in a loperamide-induced constipation model in mice. (A) Experimental protocol. (B) Orally administered **4k** or **4b** (10 mg kg⁻¹ for each) improved the three-hour stool weight, pellet number, and water content in loperamide-treated mice (mean ± S.E.M., 8–11 mice per group). Comparisons made with one-way analysis of variance with *post hoc* Newman–Keuls multiple comparisons test, **p* < 0.05, ***p* < 0.01, ****p* < 0.001, ns: not significant (*p* ≥ 0.05). ip: intraperitoneal, po: per oral.

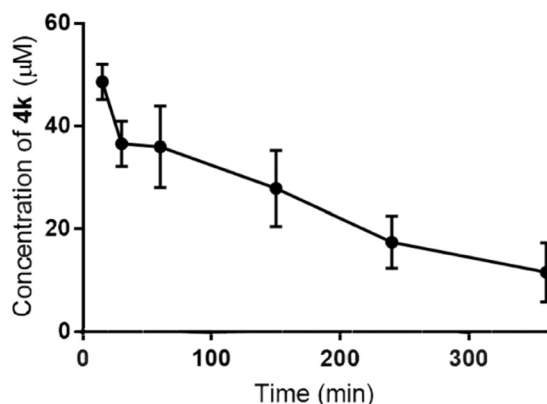


Fig. 4 4k pharmacokinetics. Serum concentration of 4k in mice at indicated time points after single dose oral administration (10 mg kg^{-1}) at zero time. Mean \pm S.E.M., $n = 4$ mice.

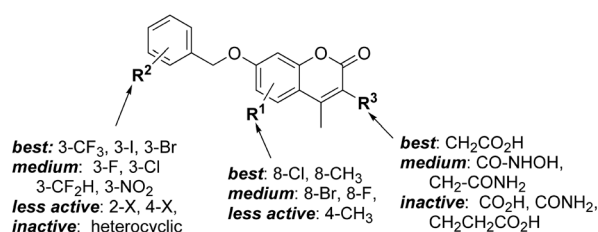


Fig. 5 Summary of SAR information identified by modifying the central coumarin substitution (R^1), benzyloxy group (R^2), and carboxylic acid (R^3) regions of the inhibitor structure. Thorough investigation of R^2 and R^3 was reported previously.¹⁸

methyl groups, and to generate new electrostatic or halogen bonding interactions with the binding site. The 8-chloro group may also enhance inhibitor lipophilicity which could lead to improved potency. We found that the 8-chloro-4-methylcoumarins (**4i–4l**) outperformed the corresponding 4,8-dimethylcoumarins (**4a–4d**) when considering different substituted benzyl groups at R^2 . Our study also showed that derivatives that contain 8-bromocoumarin (**4m–4p**) and 8-fluorocoumarin (**4q–4t**) are less potent than the corresponding 8-chlorocoumarins. The new SAR information on the coumarin core (R^1) can be integrated with results of our previous study¹⁸ that examined the benzyloxy component (R^2) and carboxylic acid appendage (R^3), to create a more complete SAR model (Fig. 5). Considering coumarin-based scaffolds more broadly, they have been shown to have anti-cancer,²⁴ anti-bacterial,²⁵ and anti-viral^{26,27} activities.

Conclusions

In conclusion, we have identified potent central 8-chloro-4-methylcoumarin containing inhibitors, **4j–4k**, with a nanomolar potency for DRA inhibition and demonstrated *in vivo* efficacy. These molecules can be used for further preclinical development as candidates for drug treatment of constipation and hyperoxaluria.

Author contributions

MA and MOA carried out the synthesis of the small molecule library, and evaluated the compounds for inhibition against DRA function. LSG performed *in vivo* characterization of compound **4k**. MOA supervised the chemistry aspects of the project, and drafted the manuscript. OC supervised the biology aspects of the project. MOA, ASV, and OC revised the manuscript. The manuscript was reviewed and approved by all authors.

Conflicts of interest

ASV and OC are inventors on patent applications, whose rights are owned by the University of California.

Acknowledgements

Supported by grants from the NIH (DK126070, DK072517, EY036139), University of California Drug Discovery Consortium, UCSF Innovation Ventures (InVent) Philanthropy Fund, NIH-NCATS through UCSF-CTSI (UL1 TR001872) and the Cystic Fibrosis Foundation. We thank Dr. Greg Elliott at the San Diego State University Mass Spectrometry Facility for high resolution mass spectrometry services.

Notes and references

- S. S. C. Rao, K. Rattanakit and T. Patcharatrakul, *Nat. Rev. Gastroenterol. Hepatol.*, 2016, **13**, 295–305.
- A. E. Bharucha, M. M. Wouters and J. Tack, *Curr. Opin. Pharmacol.*, 2017, **37**, 158–166.
- M. Camilleri, A. C. Ford, G. M. Mawe, P. G. Dinning, S. S. Rao, W. D. Chey, M. Simrén, A. Lembo, T. M. Young-Fadok and L. Chang, *Nat. Rev. Dis. Primers*, 2017, **3**, 17095.
- I. Sorokin, C. Mamoulakis, K. Miyazawa, A. Rodgers, J. Talati and Y. Lotan, *World J. Urol.*, 2017, **35**, 1301–1320.
- C. D. J. Scales, A. C. Smith, J. M. Hanley and C. S. Saigal, *Eur. Urol.*, 2012, **62**, 160–165.
- C. S. Saigal, G. Joyce and A. R. Timilsina, *Kidney Int.*, 2005, **68**, 1808–1814.
- O. Cil, T. Chu, S. Lee, P. M. Haggie and A. S. Verkman, *JCI Insight*, 2022, **7**(13), e153359.
- R. Siener, D. Ebert, C. Nicolay and A. Hesse, *Kidney Int.*, 2003, **63**, 1037–1043.
- J. C. Lieske, L. S. Peña de la Vega, J. M. Slezak, E. J. Bergstralh, C. L. Leibson, K.-L. Ho and M. T. Gettman, *Kidney Int.*, 2006, **69**, 760–764.
- S. S. Waikar, A. Srivastava, R. Palsson, T. Shafi, C.-Y. Hsu, K. Sharma, J. P. Lash, J. Chen, J. He, J. Lieske, D. Xie, X. Zhang, H. I. Feldman and G. C. Curhan, *JAMA Intern. Med.*, 2019, **179**, 542–551.
- N. Shcheynikov, Y. Wang, M. Park, S. B. H. Ko, M. Dorwart, S. Naruse, P. J. Thomas and S. Muallem, *J. Gen. Physiol.*, 2006, **127**, 511–524.
- M. R. Dorwart, N. Shcheynikov, D. Yang and S. Muallem, *Physiology*, 2008, **23**, 104–114.

- 13 S. L. Alper and A. K. Sharma, *Mol. Aspects Med.*, 2013, **34**, 494–515.
- 14 P. R. Kiela and F. K. Ghishan, *Best Pract. Res., Clin. Gastroenterol.*, 2016, **30**, 145–159.
- 15 P. Höglund, S. Haila, J. Socha, L. Tomaszewski, U. Saarialho-Kere, M. L. Karjalainen-Lindsberg, K. Airola, C. Holmberg, A. de la Chapelle and J. Kere, *Nat. Genet.*, 1996, **14**, 316–319.
- 16 C. W. Schweinfest, D. D. Spyropoulos, K. W. Henderson, J.-H. Kim, J. M. Chapman, S. Barone, R. T. Worrell, Z. Wang and M. Soleimani, *J. Biol. Chem.*, 2006, **281**, 37962–37971.
- 17 R. W. Freel, J. M. Whittamore and M. Hatch, *Am. J. Physiol.*, 2013, **305**, G520–G527.
- 18 S. Wedenoja, T. Ormälä, U. B. Berg, S. F. E. Halling, H. Jalanko, R. Karikoski, J. Kere, C. Holmberg and P. Höglund, *Kidney Int.*, 2008, **74**, 1085–1093.
- 19 P. M. Haggie, O. Cil, S. Lee, J.-A. Tan, A. A. Rivera, P.-W. Phuan and A. S. Verkman, *JCI Insight*, 2018, **3**, 121370.
- 20 S. Lee, O. Cil, P. M. Haggie and A. S. Verkman, *J. Med. Chem.*, 2019, **62**, 8330–8337.
- 21 O. Cil, M. O. Anderson, L. de Souza Goncalves, J.-A. Tan, P. M. Haggie and A. S. Verkman, *Eur. J. Med. Chem.*, 2023, **249**, 115149.
- 22 A. F. Casini, A. Pompella and M. Comporti, *Am. J. Pathol.*, 1985, **118**, 225–237.
- 23 K. Rappersberger, H. Hönigsmann, B. Ortel, A. Tanew, K. Konrad and K. Wolff, *J. Invest. Dermatol.*, 1989, **93**, 201–209.
- 24 H.-J. Lv and H.-W. Zhao, *World J. Clin. Cases*, 2020, **8**, 4958–4965.
- 25 M. Jun, A. F. Bacay, J. Moyer, A. Webb and D. Carrico-Moniz, *Bioorg. Med. Chem. Lett.*, 2014, **24**, 4654–4658.
- 26 T.-J. R. Cheng, Y.-T. Wu, S.-T. Yang, K.-H. Lo, S.-K. Chen, Y.-H. Chen, W.-I. Huang, C.-H. Yuan, C.-W. Guo, L.-Y. Huang, K.-T. Chen, H.-W. Shih, Y.-S. E. Cheng, W.-C. Cheng and C.-H. Wong, *Bioorg. Med. Chem.*, 2010, **18**, 8512–8529.
- 27 M. Z. Hassan, H. Osman, M. A. Ali and M. J. Ahsan, *Eur. J. Med. Chem.*, 2016, **123**, 236–255.